

# Phase behavior of mixtures of human lens proteins Gamma D and Beta B1

Ying Wang<sup>a</sup>, Aleksey Lomakin<sup>a</sup>, Jennifer J. McManus<sup>a,2</sup>, Olutayo Ogun<sup>a</sup>, and George B. Benedek<sup>a,b,c,1</sup>

<sup>a</sup>Materials Processing Center, <sup>b</sup>Department of Physics, and <sup>c</sup>Center for Materials Science and Engineering, Massachusetts Institute of Technology, 77 Massachusetts Avenue, Cambridge, MA 02139

Contributed by George B. Benedek, June 14, 2010 (sent for review June 1, 2010)

**We have experimentally determined the coexistence surface characterizing the phase behavior of  $\gamma$ D- $\beta$ B1-water ternary solutions. The coexistence surface fully describes the solution conditions, i.e., temperature, protein concentration, and protein composition, at which liquid-liquid phase separation occurs in a ternary solution. We have observed a significant demixing of  $\gamma$ D and  $\beta$ B1 i.e., large difference of composition in the two coexisting phases. This demixing suggests that the energy of the  $\gamma$ D- $\beta$ B1 attractive interaction is significantly smaller than the energy of the  $\gamma$ D- $\gamma$ D attractive interaction. We also observed the lowering of the phase separation temperature upon increasing of the fraction of  $\beta$ B1 in solution. We provide a theoretical analysis of our experimental data, which enables a quantitative description of our principal experimental findings. In this way, we have evaluated the magnitude and temperature dependence of the relevant interprotein interaction energies. Our findings provide insight into the factors essential for maintaining lens proteins in a single homogeneous phase, thereby enabling lens transparency.**

cataract | crystallin | phase separation | mixture

The cytoplasm of eye lens fiber cells contains a concentrated multicomponent mixture of predominantly crystallin proteins (1, 2). Crystallins were classified into three categories:  $\alpha$ ,  $\beta$ , and  $\gamma$  crystallin (3). The  $\beta$  and  $\gamma$  crystallins have a common polypeptide chain fold and together form a super family of  $\beta$ - $\gamma$  crystallins. To maintain lens transparency this multicomponent mixture must be free of large density variations, which produce light scattering. Conversely, inhomogeneities in the protein density produced by aggregation and phase transitions can lead to cataract (4, 5).

Aggregation and phase transitions of aqueous solutions of protein mixtures are generally driven by attractive interprotein interactions (6, 7). A large body of work has been devoted to studies of interprotein interactions in single component aqueous solutions of eye lens proteins (8–13). In order to obtain further insight into maintenance of transparency in eye lens, aqueous solutions of crystallin mixture with high concentration must also be investigated. Observation of liquid-liquid phase separation (LLPS) in protein solutions provides a direct tool to probe collective interprotein interaction at concentrations up to 400 mg/mL (which is approximately the total protein concentration in a human eye lens) (14–17). Significant researches have been conducted on the LLPS of solutions of crystallin mixtures. LLPS of mixtures of different types of bovine  $\gamma$  crystallins has been thoroughly investigated (14, 15). Recently, phase separation of  $\alpha$ - $\gamma$  mixtures was also studied (18, 19).

Due to the abundances of  $\beta$  (~50% of eye lens protein) and  $\gamma$  (~20%) crystallins in human eye lens (20), studies of their mixtures are of particular importance. In relation to cataract disease,  $\gamma$ D and  $\beta$ B1 are two especially interesting members of the  $\beta$ - $\gamma$  crystallin family. Mutations of  $\gamma$ D crystallin are found in many types of hereditary cataracts (9–12, 21).  $\beta$ B1 is subjected to extensive age-related modifications such as N terminus truncation and deamidation, and it occurs in large amounts in the age associated cataracts (20). Here, we present a study of the LLPS of mixtures of human  $\gamma$ D and  $\beta$ B1 crystallin in aqueous solution.

In this work, the numbers of  $\gamma$ D and  $\beta$ B1 molecules in a ternary solution are respectively denoted by  $N_1$  and  $N_2$ . The total protein “concentration”  $\phi$ , can be defined as the volume fraction of proteins, where  $(N_1 + N_2)\Omega_p/V$ . Here  $V$  is the solution volume, and  $\Omega_p$  is the effective volume of a single globular protein molecule, which we will assume to be the same for  $\gamma$ D and  $\beta$ B1 crystallins (8, 22). We will refer to the mole fraction of  $\beta$ B1,  $x = N_2/(N_1 + N_2)$ , as the protein “composition” of this solution.

A thermodynamic state of  $\gamma$ D- $\beta$ B1-water ternary solutions can be fully determined using three state variables ( $T, \phi, x$ ) where  $T$  is the solution temperature. The LLPS of a solution with a particular  $\phi$  and  $x$  occurs at a well defined temperature  $T_{ph}$ , which is a function of  $\phi$  and  $x$ . Therefore, LLPS of  $\gamma$ D- $\beta$ B1-water ternary solution is described by a coexistence surface,  $T_{ph}(\phi, x)$ , in the three-dimensional ( $T, \phi, x$ ) coordinate space. In this work, we experimentally constructed this coexistence surface by measuring the cloud point curves,  $T_{ph}(\phi)$ , i.e., the constant  $x$  cross-sections, at several different  $x$ . We also experimentally determined the constant  $T_{ph}$  cross-sections of the coexistence surface,  $x(\phi)_{T_{ph}}$ , known as binodal curves, at different  $T_{ph}$ . Upon LLPS at given  $T_{ph}$ , the initially homogeneous protein solution will separate into a protein-poor phase (phase I) with small  $\phi^I$  and protein-rich phase (phase II) with large  $\phi^{II}$ . A binodal curve consists of pairs of points representing protein concentrations and compositions of protein-poor phases ( $\phi^I, x^I$ ) and protein-rich phases ( $\phi^{II}, x^{II}$ ) coexisting at given  $T_{ph}$ . The line connecting a pair of points is called a tie-line. At the so called critical point the difference between composition and concentration of the coexisting phases becomes infinitesimally small i.e., the tie-line length becomes zero, and the direction of tie-line becomes tangential to the binodal curve. The set of critical points form a critical line on the coexistence surface.

Generally, LLPS of a ternary protein solution involves “protein condensation” and “protein demixing.” Protein condensation refers to the formation of two phases with different total protein concentration,  $\phi$ . This concentrational separation is analogous to the “usual” LLPS of a protein-water binary solution. Protein demixing refers to the formation of two phases with differing protein compositions,  $x$ . The relative importance of protein condensation and protein demixing in LLPS of any specific two proteins-water ternary system depends on the characteristics of the interprotein interactions.

In a  $\gamma$ D- $\beta$ B1-water ternary solution, the interprotein interactions are described by three effective energies of pair-wise interaction:  $E_{11}$  for a  $\gamma$ D- $\gamma$ D pair,  $E_{12}$  for a  $\gamma$ D- $\beta$ B1 pair, and  $E_{22}$  for a  $\beta$ B1- $\beta$ B1 pair. To observe LLPS in a protein-water binary system

Author contributions: Y.W., A.L., and G.B.B. designed research; Y.W., J.J.M., and O.O. performed research; Y.W., A.L., and G.B.B. analyzed data; and Y.W., A.L., and G.B.B. wrote the paper.

The authors declare no conflict of interest.

<sup>1</sup>To whom correspondence may be addressed. E-mail: benedek@mit.edu or ywang09@mit.edu.

<sup>2</sup>Present address: Department of Chemistry, NUI Maynooth, Maynooth, County Kildare, Ireland.

This article contains supporting information online at [www.pnas.org/lookup/suppl/doi:10.1073/pnas.1008353107/-DCSupplemental](http://www.pnas.org/lookup/suppl/doi:10.1073/pnas.1008353107/-DCSupplemental).

the interprotein interactions must be attractive i.e., the corresponding  $E_{11}$  or  $E_{22}$  must be negative. In such a binary solution, the maximum LLPS temperature ( $T_c$ ) is directly proportional to the magnitude of the interprotein interaction. Since  $T_c$  of the  $\gamma$ D-water binary solution is around 277 K (10), while  $T_c$  of the  $\beta$ B1-water binary solution is around 249 K (8), it follows that the magnitude of  $E_{11}$  is larger than that of  $E_{22}$ . As  $x$  increases from 0, some  $\gamma$ D- $\gamma$ D contacts with energy  $E_{11}$  are replaced by  $\gamma$ D- $\beta$ B1 contacts with energy  $E_{12}$ . Since  $x$  is relatively small under our experimental condition the number of  $\beta$ B1- $\beta$ B1 contacts is negligible. The difference in contact energies  $E_{12}$  and  $E_{11}$  drives demixing. When the magnitude of  $E_{12}$  is smaller than that of  $E_{11}$ ,  $\beta$ B1 is repelled from the  $\gamma$ D protein-rich phase. When  $\beta$ B1 preferentially partitions into the protein-dilute phase, adding  $\beta$ B1 lowers the LLPS temperature of the  $\gamma$ D solution. This phenomenon is analogous to the suppression of the freezing point by adding a solute into water. Indeed, in our experiments we observed and measured both reduction of phase separation temperature and strong protein demixing. We present a theoretical analysis, which provides a quantitative interpretation of our data.

## Results

**Dependence of  $T_{ph}$  on  $\phi$  at Fixed  $x$ .** In Fig. 1 we present the results of the measurements of the cloud point curves  $T_{ph}(\phi)_x$ , i.e., the constant  $x$  sections of the coexistence surface.  $T_{ph}(\phi)_x$  is reported at  $x = 0, 0.08, 0.16$ , and  $0.29$ . The entire cloud point curve shifts to lower temperature as  $x$  increases. For ternary mixtures with  $x > 0.29$ , phase separation cannot be observed because  $T_{ph}$  falls below the freezing point of the solutions. The  $\phi$  value at which  $T_{ph}$  is maximal first decreases and then increases with increasing  $x$ .

The clouding of the solution upon lowering the temperature occurs at lower temperatures than the clarification that occurs upon temperature rise. This hysteresis is shown in Fig. 1 by vertical bars between clouding and clarification temperatures. The hysteresis is a nonequilibrium phenomenon that depends on the rate of sample cooling and heating and also on the kinetics

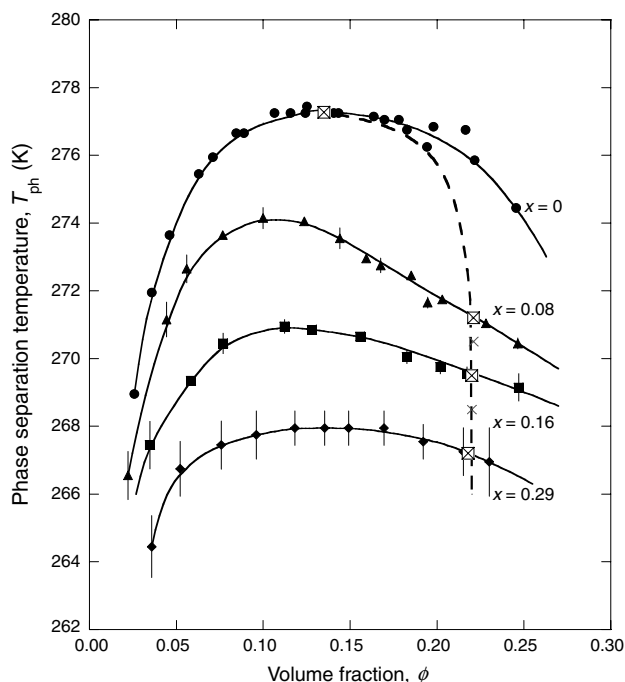


**Fig. 1.**  $T_{ph}(\phi)$ 's are presented at  $x = 0$  (circles),  $0.08$  (triangles),  $0.16$  (squares), and  $0.29$  (diamonds). Solid curves are eye guides for the cloud point curves  $T_{ph}(\phi)_x$ . Vertical bars represent the hysteresis. The projection of the critical point line to the constant  $x$  plane is represented by the dashed curve. The intersections of critical line and cloud point curves are marked by the crossed squares.

of relaxation processes in the solution such as nucleation rate of droplets of the condensed phase, merging or sedimentation of droplets, and possible crystallization. This hysteresis is the main source of uncertainty in determination of  $T_{ph}$ . At the same time the hysteresis can provide qualitative information on the nucleation rate of droplets of the condensed phase. In the  $\gamma$ D-water binary system the observed hysteresis was too small to be seen in Fig. 1. (When the  $\gamma$ D volume fraction was below  $\sim 0.1$ , the emerging droplets sedimented too fast for the clarifying temperature to be measured. See *Materials and Methods*) Upon adding  $\beta$ B1, hysteresis increases as shown in Fig. 1. This observation implies that the presence of  $\beta$ B1 increases the nucleation energy barrier for formation of droplets in bulk solutions.

The positions of the critical points on these cloud point curves are shown in Fig. 1. In protein-water binary systems, the critical point is at the maximum of the cloud point curve (23, 24). Here, the critical point of the  $\gamma$ D-water binary solution is at  $\phi_c = 0.13 \pm 0.01$  and  $T_c = 277.3 \pm 0.1$  K. At  $x > 0$ , the critical points are not necessarily located at the maxima of  $T_{ph}(\phi)_x$  curves, and cannot be determined solely from cloud point measurements. The projection of the critical line shown in Fig. 1 is derived from the results of partitioning measurements described in the next section.

**Binodal Curves of Coexisting Phases at Constant  $T_{ph}$ .** In Fig. 2, we present the results of partitioning measurements. Protein concen-

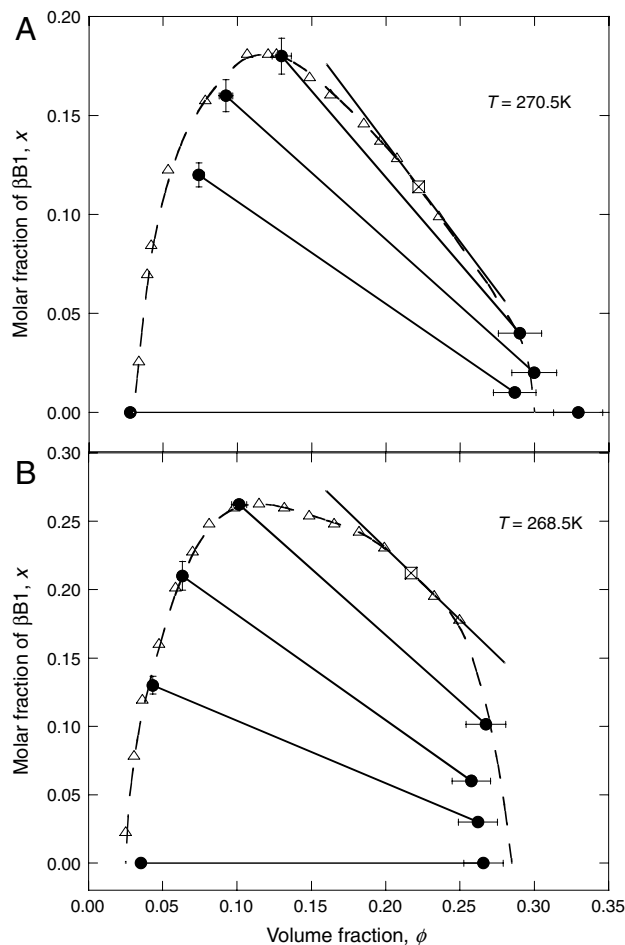


**Fig. 2.** Isothermal cross-sections of coexistence surface at  $T_{ph} = 270.5$  K (A) and  $268.5$  K (B). The solid lines are tie-lines which connect pairs of points (solid circles) representing coexisting protein-rich and protein-poor phases in partitioning measurements. Dashed lines are eye guides for the binodal curves through data points of cloud-point measurements (open triangles) and partitioning measurements. The critical points are represented by crossed squares.

trations and compositions of coexisting protein-poor phase ( $\phi^I, x^I$ ) and protein-rich phase ( $\phi^{II}, x^{II}$ ) are reported at  $T_{ph} = 270.5$  K and 268.5 K. Each pair of points for coexisting phases is connected by tie-lines. The slopes of tie-lines characterize the relative importance of protein condensation and demixing to LLPS. The horizontal tie-line signifies no demixing. The slopes of tie-lines are negative and significantly increase, as the proportion of  $\beta B1$  increases.

In the vicinity of the critical point, the pairs of points on binodal curve that correspond to coexisting phases are difficult to determine by partitioning measurements, due to the slow dynamics of LLPS, and the small difference between coexisting phases. The binodal curve,  $x(\phi)_{T_{ph}}$ , here can be determined more accurately by interpolating the cloud point data,  $T_{ph}(\phi)_x$ . The points deduced from such interpolation are presented in Fig. 2. The two sets of data from partitioning measurements and from  $T_{ph}$  measurements are consistent within experimental error. Because the two coexisting phases coincide at the critical point, the position of the critical point ( $\phi_c, x_c$ ) at a given temperature can be estimated by extrapolating tie-lines to  $\phi^{II} = \phi^I = \phi_c$ , on the  $x(\phi)_{T_{ph}}$  boundary as described in the Discussion section. At  $T_{ph} = 270.5$  K,  $x_c = 0.11 \pm 0.01$ , and  $\phi_c = 0.22 \pm 0.01$ . At  $T_{ph} = 268.5$  K,  $x_c = 0.21 \pm 0.01$ ,  $\phi_c = 0.22 \pm 0.01$ .

While conducting partitioning measurements, after two weeks of incubation, we observed many crystals in the protein-rich bottom phase. These crystals have a rhombus shape (Fig. 3) identical to the geometry of crystals formed in the  $\gamma D$  solutions (25), and we believe that these indeed are  $\gamma D$  crystals. The formation of crystals implies that  $\gamma D$  can readily crystallize in mixtures with  $\beta B1$  and confirms that LLPS is metastable with respect to crystallization and that LLPS facilitates crystallization (17, 26).

**Coexistence Surface of  $\gamma D$ - $\beta B1$ -Water Ternary Solution.** In Fig. 4 we show the coexistence surface of the  $\gamma D$ - $\beta B1$  system reconstructed from both cloud point measurements and partitioning experiments. The coexistence surface, at each point, is described by three derivatives:  $(\partial T_{ph}/\partial \phi)_x$ ,  $(\partial T_{ph}/\partial x)_\phi$ , and  $(\partial x/\partial \phi)_{T_{ph}}$ . These three derivatives are related mathematically by:

$$(\partial T_{ph}/\partial \phi)_x = -(\partial T_{ph}/\partial x)_\phi (\partial x/\partial \phi)_{T_{ph}} \quad [1]$$

In Fig. 4, we observe that  $(\partial T_{ph}/\partial x)_\phi$  is always negative. Thus, according to Eq. 1,  $(\partial x/\partial \phi)_{T_{ph}}$  and  $(\partial T_{ph}/\partial \phi)_x$  always have the same sign, and  $(\partial x/\partial \phi)_{T_{ph}}$  must be equal to zero when  $(\partial T_{ph}/\partial \phi)_x$  is equal to zero. Thus, the line of maxima of the cloud point curves coincides with the line where the binodal curves have maxima. This “ridge line” on the coexistence surface is shown as the red dashed line in Fig. 4. On the lower  $\phi$  side of the ridge line, both  $(\partial x/\partial \phi)_{T_{ph}}$  and  $(\partial T_{ph}/\partial \phi)_x$  are positive. On the higher  $\phi$

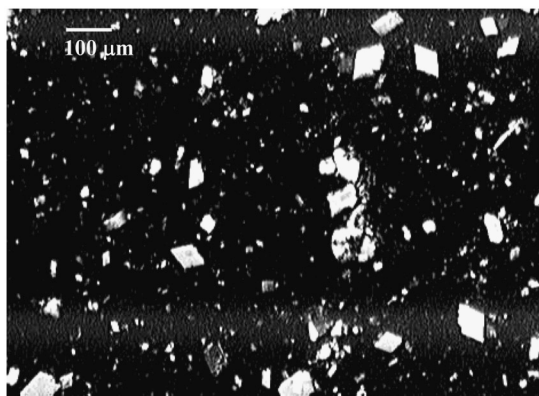


**Fig. 3.** Polarization microscopy image of  $\gamma D$  crystals. Crystals were taken from the protein-rich phase ( $\phi = 0.27$  and  $x = 0.11$ ) in a partitioning measurement after two weeks incubation at 268.5 K. Image was taken at room temperature.

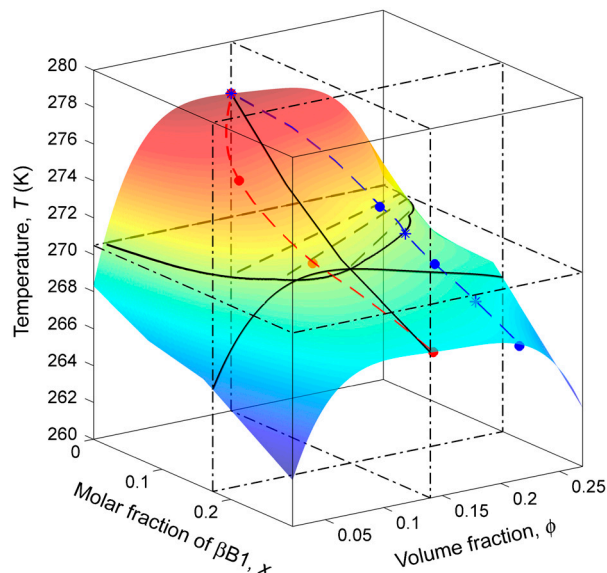


**Fig. 4.** Illustration of LLPS coexisting surface of  $\gamma D$ - $\beta B1$ -water ternary system. The colors from red to blue indicate the  $T_{ph}$  gradient on the coexistence surface from high to low temperature. The black solid lines are representative cross-sections of the coexistence surface at constant  $\phi$ ,  $x$ , and  $T_{ph}$ . The black dashed lines represent tie-lines of coexisting phases in a constant  $T_{ph}$  plane. The red dashed line is the eye guide for the ridge line drawn through the experimental maximum points (red circles) in cloud-point measurements. The blue dashed line is the eye guide for the critical point line drawn through the experimental critical points (blue circles).

side, these two derivatives are both negative. Interestingly, in the low  $\phi$  region ( $\phi < \sim 0.1$ ),  $T_{ph}$  with good accuracy is a linear function of  $x$ , as shown in Fig. 5. The extrapolation of  $T_{ph}$  to 100%  $\beta B1$  solution, i.e.,  $x = 1$ , agrees well with  $T_{ph} = 249 \pm 2$  K of pure  $\beta B1$  solutions (8).

We know experimentally critical points ( $\phi^c, x^c$ ) at three different temperatures: at  $T_{ph} = 277.3$  K, from the position of the maximum on the coexistence curve in the pure  $\gamma D$  solution (Fig. 1), and at  $T_{ph} = 270.5$  K, and  $T_{ph} = 268.5$  K, from the critical points on the binodal lines (Fig. 2). Using these three points we can draw the curve of  $T_{ph}(\phi^c, x^c)$ , and determine the location of the critical points on each of the cloud point curves (Fig. 4). We observe that the critical line is significantly shifted from the ridge line toward large  $\phi$ . This observation is the result of strong demixing effects. The derivative  $(\partial x/\partial \phi)_{T_{ph}}$  is negative, signifying preferential partitioning of  $\beta B1$  into the protein-poor phase, and its magnitude increases with  $x$ .

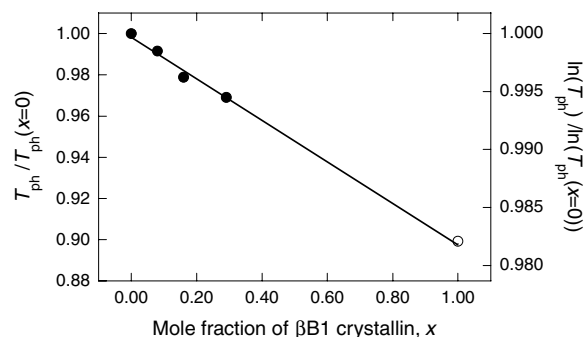


**Fig. 5.**  $T_{ph}$  of a  $\gamma D$ - $\beta B1$  mixture solution at  $\phi = 0.071$  and different  $x$ .  $T_{ph}$  (left vertical axis) and natural logarithm of  $T_{ph}$  (right vertical axis) are plotted as a function of  $\beta B1$  crystallin fractions,  $x$ , as the solid circles. The open circle represents  $T_{ph}$  and logarithm of  $T_{ph}$  of pure  $\beta B1$  solution deduced from  $\beta B1$ -PEG-water ternary system.



**Quasielastic Light-Scattering (QLS) Studies of  $\gamma$ D- $\beta$ B1 Mixtures.** To characterize the size and interprotein interaction of proteins in  $\gamma$ D- $\beta$ B1 solutions we have conducted QLS experiments. We first measured the diffusion coefficients,  $D$ 's, of proteins in both pure  $\gamma$ D solution and pure  $\beta$ B1 solution. The corresponding hydrodynamic radii were calculated using Stokes-Einstein relation:  $R_h = kT/6\pi\eta D$ , where  $k$  is Boltzmann's constant and  $\eta$  is the viscosity of buffer solution. The hydrodynamic radius,  $R_{h1}$ , of pure  $\gamma$ D is  $2.3 \pm 0.1$  nm, and  $R_{h2}$  of pure  $\beta$ B1 monomer is  $3.0 \pm 0.1$  nm (8). The difference in hydrodynamic size is mostly due to the extended terminal arms of  $\beta$ B1, as the globular body of  $\beta$ B1 is known to be about the same as that of  $\gamma$ D (8). We have also obtained the average  $R_h$ 's in solutions with different proportion of  $\beta$ B1:  $R_h$  is equal to  $2.3 \pm 0.1$  nm at  $x = 0.04$  and  $2.4 \pm 0.1$  nm at  $x = 0.08$ . These values are equal to the values of  $R_h(x)$  calculated from the z-average of diffusion coefficients of  $\gamma$ D and  $\beta$ B1 monomers, i.e.,  $D(x) = ((1-x)M_1^2D_1 + xM_2^2D_2)/((1-x)M_1^2 + xM_2^2)$ , where  $M_1$  and  $M_2$  are respectively the molecular weights of  $\gamma$ D and  $\beta$ B1. This equality indicates that aggregation, including homodimerization of  $\beta$ B1, is negligible in our experiments.

In order to characterize the interprotein interactions in  $\gamma$ D- $\beta$ B1 solution, the apparent diffusion coefficients in solutions with different proportions of  $\beta$ B1 ( $x = 0, 0.04, \text{ and } 0.08$ ) were measured as a function of  $\phi$ . Within the concentration range of measurement ( $0.002 \leq \phi \leq 0.021$ ),  $D$  decreases linearly with  $\phi$  (Fig. 6). The large negative slope,  $(dD/d\phi)_x < 0$ , implies a net effective attractive interaction between the protein molecules in these solutions. The decrease in magnitude of this slope as  $x$  increases suggests that the net effective attractive interprotein interaction in solution is reduced by adding  $\beta$ B1. This observation is in accordance with the reduction  $T_{ph}$  by adding  $\beta$ B1.

### Discussion

The coexistence surface of the  $\gamma$ D- $\beta$ B1-water ternary solution can be theoretically derived if the expression for the free energy is known.  $\gamma$ D and  $\beta$ B1 crystallins are globular proteins of approximately the same geometrical size (8). The QLS measurements showed that  $\beta$ B1 crystallin in solutions with relatively low  $\phi$  and  $x$  is in monomer form. We assume here that at our relatively low concentrations of  $\beta$ B1 the role of oligomerization of  $\beta$ B1 is negligible and our  $\gamma$ D- $\beta$ B1-water solutions can be treated as a colloidal mixture of two spherical components with the same size. In thermodynamic analysis, an incompressible solution of particles is equivalent to a compressible fluid constituted of the solute particles at pressure equal to the osmotic pressure,  $\Pi$ , in the solution (27). We therefore introduce a reduced Gibbs free energy

$g(\Pi, T, x) \equiv G(\Pi, T, N_1, N_2)/N$ . Here,  $N = N_1 + N_2$ , where  $N_1$  and  $N_2$  are respectively the numbers of  $\gamma$ D and  $\beta$ B1 molecules. For a colloid mixture of two distinct spherical components with the same size, the reduced Gibbs free energy can be written as:  $g = kTs_{HS} + kTs_{mix} + U$ . Here  $s_{HS}$  is the entropy per particle in a solution of hard-spheres, which is well approximated by the Carnahan Starling expression (28):  $s_{HS} = \ln \phi + (1 + 5\phi - 6\phi^2 + 2\phi^3)/(1 - \phi)^3$ .  $s_{mix}$  is the entropy per particle of mixing two distinguishable proteins:  $s_{mix} = x \ln x + (1 - x) \ln(1 - x)$ .  $U$  is the free energy associated with interprotein interactions.  $U$  is a function of the state variables:  $\Pi$ ,  $T$ , and  $x$ .

Let us first consider a  $\gamma$ D-water binary solution,  $x = 0$ . In this case,  $g$  is the chemical potential of  $\gamma$ D, and  $U$  is the energy needed to remove one  $\gamma$ D molecule from the solution. This energy,  $U$ , can be viewed as a product of the average number of contacts,  $n_c$ , times the effective energy,  $E_{11}$ , per contact between  $\gamma$ D molecules, i.e.,  $U = n_c E_{11}$ . Of course, the notion of a "contact" is unambiguous only in the framework of the square-well potential model with a specific range of interaction. Nevertheless, the number of contacts has proven to be a useful concept for understanding the phase behavior of colloid systems (24, 29). Generally,  $U$  is a function of the temperature. However, a solution of globular proteins can be regarded as a colloid system with relatively weak interactions. In such systems the spatial distribution function and thus  $n_c$  is mainly governed by entropic excluded volume interaction, and therefore  $n_c$  would be independent of temperature. In effect, we describe the thermodynamic features of our system in a high temperature approximation (30). Hereafter,  $n_c$  is dependent only on the volume fraction,  $\phi$ , which here has to be treated as a function of osmotic pressure,  $\Pi$ . Note that the effective free energy of a contact between protein molecules,  $E_{11}$ , may have an entropic component and thus can be temperature dependent.

In a  $\gamma$ D- $\beta$ B1-water ternary solution,  $x > 0$ , some of the  $\gamma$ D molecules are replaced by  $\beta$ B1 molecules of the same size, but with different contact energy,  $E_{12}$ . In the same high temperature approximation as described above,  $n_c$  is not affected by interparticle interactions. Thus the change of total contact energy associated with a replacement of  $\gamma$ D with  $\beta$ B1 will be  $n_c(E_{12} - E_{11})$ . Therefore, when  $x$  is small and the contacts of  $\beta$ B1 molecules with each other can be ignored, we can model  $U$  as  $U = n_c(E_{11} + x(E_{12} - E_{11}))$ .

Having defined all the terms of the Gibbs free energy, we can now calculate the chemical potentials of the two proteins in the solution:  $\mu_1 \equiv (\partial G/\partial N_1)_{N_2, \Pi, T}$  and  $\mu_2 \equiv (\partial G/\partial N_2)_{N_1, \Pi, T}$  to the lowest order in  $x$ :

$$\mu_1 = kTs_{HS} + n_c E_{11} - kTx \quad [2a]$$

$$\mu_2 - \mu_1 = kT \ln x + n_c(E_{12} - E_{11}). \quad [2b]$$

The coexistence surface is defined by a set of two equations which express the equality of the chemical potentials of  $\gamma$ D and  $\beta$ B1 molecules in two phases:

$$\mu_1^I(\Pi, T, x^I) = \mu_1^{II}(\Pi, T, x^{II}) \quad [3a]$$

$$\mu_2^I(\Pi, T, x^I) - \mu_1^I(\Pi, T, x^I) = \mu_2^{II}(\Pi, T, x^{II}) - \mu_1^{II}(\Pi, T, x^{II}). \quad [3b]$$

Below, we discuss two specific features of the coexistence surface, namely the slope of tie-lines and the  $T_{ph}$  dependence on  $x$ , both of which can be quantitatively analyzed even without explicit knowledge of  $n_c(\phi)$ .

**Slope of Tie-Lines.** An important experimentally observed feature of  $\gamma$ D- $\beta$ B1 solutions is that the slopes of tie-lines in the isotherm cross-section (Fig. 2) have negative values with magnitudes increasing as the average  $x$  increases. The negative slope of the

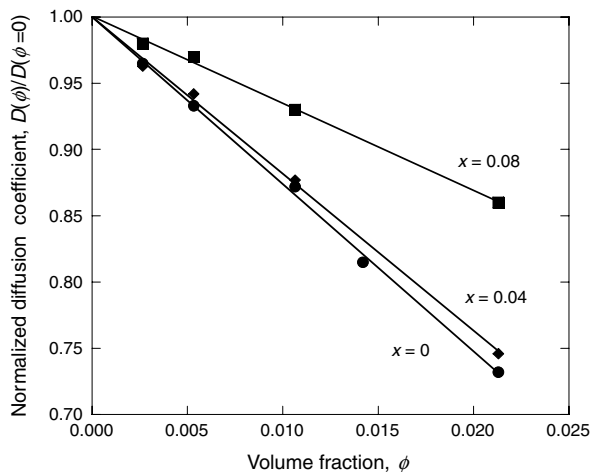


**Fig. 6.** Normalized diffusion coefficients  $D(\phi)/D(\phi = 0)$  are plotted as a function of volume fraction  $\phi$ , for  $\gamma$ D solution (circles) and  $\gamma$ D- $\beta$ B1 mixture solutions with  $x = 0.04$  (diamonds) and  $0.08$  (squares).

tie-lines signifies that  $\beta$ B1 is expelled from the dense  $\gamma$ D phase. Because the  $x$ 's are small and thus  $\beta$ B1- $\beta$ B1 interaction is negligible, this observation implies that the effective  $\gamma$ D- $\beta$ B1 interaction is less attractive than the  $\gamma$ D- $\gamma$ D interaction, i.e.,  $|E_{12}| < |E_{11}|$ . To quantify the slope of tie-lines we substitute Eq. 2b into Eq. 3b and find:

$$kT_{\text{ph}}(\ln x^{\text{II}} - \ln x^{\text{I}}) = -(n^{\text{II}} - n^{\text{I}})(E_{12} - E_{11}), \quad [4]$$

where  $n^{\text{I}} = n_c(\phi^{\text{I}})$  and  $n^{\text{II}} = n_c(\phi^{\text{II}})$ . Note that when phase separation occurs, the two coexisting phases, while having the same osmotic pressure, have two different values of  $\phi$  and thus two different values of  $n_c(\phi)$ . Substituting Eq. 2a into Eq. 3a we find to the lowest order of  $x$ :

$$kT_{\text{ph}}(s_{\text{HS}}^{\text{II}} - s_{\text{HS}}^{\text{I}}) = -(n^{\text{II}} - n^{\text{I}})E_{11}, \quad [5]$$

where  $s_{\text{HS}}^{\text{I}} = s_{\text{HS}}(\phi^{\text{I}})$  and  $s_{\text{HS}}^{\text{II}} = s_{\text{HS}}(\phi^{\text{II}})$ . Combining Eq. 4 and Eq. 5, we can obtain the relation between the steepness of a tie-line and the energies of interprotein interaction:

$$(E_{12} - E_{11})/E_{11} = (\ln x^{\text{II}} - \ln x^{\text{I}})/(s_{\text{HS}}^{\text{II}} - s_{\text{HS}}^{\text{I}}). \quad [6]$$

Using the Carnahan Starling expression for  $s_{\text{HS}}(\phi)$ , we substitute the experimental data for  $(\phi^{\text{I}}, x^{\text{I}})$  and  $(\phi^{\text{II}}, x^{\text{II}})$  shown in Fig. 2 into Eq. 6, and calculate values of  $E_{12}/E_{11}$  corresponding to each tie-line. These values are shown in Table 1.  $E_{12}/E_{11}$  is equal to  $0.59 \pm 0.02$  at 270.5 K and is equal to  $0.73 \pm 0.03$  at 268.5 K. We comment that a difference between the values of  $E_{12}/E_{11}$  at different temperatures can be expected due to the anisotropy of interprotein interactions and other entropic contributions which lead to a temperature dependence of the effective interaction energies (24, 29). The ratio  $E_{12}/E_{11}$  is a robust physical quantity which determines the steepness of tie-line. In contrast, the absolute magnitudes of the contact energies are model dependent and only the product,  $n_c E_{11}$ , is physically significant. Nevertheless, it can be said that  $E_{11}$  has a negative value, of the order of  $kT_c$ .

With  $E_{12}/E_{11}$  known, we used Eq. 6 together with the experimentally determined binodal curve,  $x(\phi)_{T_{\text{ph}}}$ , to determine for any  $(\phi^{\text{I}}, x^{\text{I}})$  the corresponding  $(\phi^{\text{II}}, x^{\text{II}})$ . This approach enables the construction of a family of tie-lines which can be extrapolated to the vicinity of the critical point ( $x^{\text{I}} \rightarrow x^{\text{II}}$  and  $\phi^{\text{I}} \rightarrow \phi^{\text{II}}$ ) on the binodal curve. We used this procedure to graphically locate the critical points shown in Fig. 2.

**Reduction of Phase Separation Temperature upon Adding  $\beta$ B1 Crystallin.** To calculate the reduction of  $T_{\text{ph}}$  upon increasing  $\beta$ B1 fraction, i.e.,  $\Delta T_{\text{ph}}(x)$ , we compare Eq. 3a written at some fixed osmotic pressure for a  $\gamma$ D-water binary solution with that for a  $\gamma$ D- $\beta$ B1-water ternary solution. Omitting the fixed variable  $\Pi$  we can write  $\mu_1^{\text{I}}(T_{\text{ph}}, 0) = \mu_1^{\text{II}}(T_{\text{ph}}, 0)$  for pure  $\gamma$ D and  $\mu_1^{\text{I}}(T_{\text{ph}} + \Delta T_{\text{ph}}, x^{\text{I}}) = \mu_1^{\text{II}}(T_{\text{ph}} + \Delta T_{\text{ph}}, x^{\text{II}})$  for the  $\gamma$ D- $\beta$ B1 mixture. Expanding the second condition to the first order in  $\Delta T_{\text{ph}}$  and in  $x$  around  $T = T_{\text{ph}}$  and  $x = 0$ , we obtain a general formula for the change of phase transition temperature upon adding a small amount of second component (31):

$$(\Delta T_{\text{ph}})_{\Pi} = \frac{kT_{\text{ph}}(x^{\text{I}} - x^{\text{II}})}{\partial \mu_1^{\text{I}}/\partial T - \partial \mu_1^{\text{II}}/\partial T} = \frac{kT_{\text{ph}}^2(x^{\text{I}} - x^{\text{II}})}{q}. \quad [7]$$

**Table 1.  $E_{12}/E_{11}$  calculated from the tie-lines shown in Fig. 2**

$T_{\text{ph}}$	$\phi^{\text{I}}$	$\phi^{\text{II}}$	$x^{\text{I}}$	$x^{\text{II}}$	$E_{12}/E_{11}$
270.5	0.07	0.29	0.12	0.01	0.58
270.5	0.09	0.30	0.16	0.02	0.61
270.5	0.13	0.29	0.18	0.03	0.59
268.5	0.04	0.26	0.13	0.03	0.72
268.5	0.06	0.26	0.21	0.06	0.72
268.5	0.10	0.27	0.26	0.10	0.76

We used here  $\partial \mu_1/\partial x = -kT_{\text{ph}}$ , according to Eq. 2a. Because  $\partial \mu_1/\partial T$  is the entropy per molecule,  $q$  is the molecular latent heat of LLPS of the  $\gamma$ D-water binary solution. According to Eq. 2a,  $q = kT_{\text{ph}}(s_{\text{HS}}^{\text{I}} - s_{\text{HS}}^{\text{II}}) + (n^{\text{I}} - n^{\text{II}})T_{\text{ph}}(dE_{11}/dT)$ . This latent heat,  $q$ , consists of two components: the first one,  $kT_{\text{ph}}(s_{\text{HS}}^{\text{I}} - s_{\text{HS}}^{\text{II}})$ , is associated with the entropy change due to excluded volume; the second one,  $(n^{\text{I}} - n^{\text{II}})T_{\text{ph}}(dE_{11}/dT)$ , is the difference in entropic components of the effective interprotein interaction.

Eq. 7 gives an expression for the temperature shift at fixed osmotic pressure while the experimentally determined quantity is the temperature shift at constant concentration. In the dilute phase  $\phi^{\text{I}} \ll 1$ , where  $\Pi \approx kT\phi^{\text{I}}$ , the relative difference between  $(\Delta T_{\text{ph}})_{\phi}$  and  $(\Delta T_{\text{ph}})_{\Pi}$  is:  $((\Delta T_{\text{ph}})_{\phi} - (\Delta T_{\text{ph}})_{\Pi})/(\Delta T_{\text{ph}})_{\Pi} = (\partial T_{\text{ph}}/\partial \phi)(\phi/T_{\text{ph}})$ . This difference is numerically less than 2% and can be neglected. Furthermore, in the  $\gamma$ D- $\beta$ B1 mixture, the  $\beta$ B1 predominantly partitions into protein-poor phase I, i.e.,  $x^{\text{I}} \gg x^{\text{II}}$ . Thereby, using Eq. 5 for the expression of  $(n^{\text{I}} - n^{\text{II}})$ , we find:

$$(\Delta T_{\text{ph}})_{\phi}/T_{\text{ph}} \approx \frac{kT_{\text{ph}}x^{\text{I}}}{q} = \frac{x^{\text{I}}}{(s_{\text{HS}}^{\text{I}} - s_{\text{HS}}^{\text{II}})[1 - (dE_{11}/dT)(T_{\text{ph}}/E_{11})]}. \quad [8]$$

Eq. 8 allows us to determine the latent heat of LLPS,  $q$ , and the entropic component of interprotein interaction in a pure protein-water solution,  $(dE_{11}/dT)T/E_{11}$ . By simultaneously fitting the experimental  $(\Delta T_{\text{ph}}(x))_{\phi}$  in Fig. 1 at several different  $\phi^{\text{I}}$ 's (Fig. S1), we find  $(dE_{11}/dT)T/E_{11} = -1.0 \pm 0.2$ . This value signifies that the entropic component of the  $\gamma$ D- $\gamma$ D interaction is comparable to the excluded volume entropy. The values of  $q$ 's at concentrations used in the fitting procedure are listed in Table 2. The negative value of  $q$  is consistent with the idea that  $\beta$ B1 suppresses the phase separation temperature and thereby plays the role of phase separation inhibitor. The  $T_{\text{ph}}$  reduction ( $\sim 7^\circ\text{C}$  with  $x \approx 0.3$ ) due to demixing that occurs during  $\gamma$ D- $\beta$ B1 phase separation is comparable to the effect of previously discovered small molecule cataract inhibitors (32, 33) which, at high mole fractions,  $x$ , up to 0.66, chemically modify eye lens proteins. Our analysis suggests that the solution components which undergo strong demixing from the major eye lens proteins serve as important agents which may forestall a cataractogenic phase transition. Such strongly demixing agents could be viable guides in the design of cataract inhibiting drugs.

In conclusion, we have experimentally determined the LLPS coexistence surface of the  $\gamma$ D- $\beta$ B1-water ternary system. Two important features were observed: (i) strong demixing of  $\gamma$ D and  $\beta$ B1, with  $\beta$ B1 preferentially segregated into the dilute phase; (ii) a significant decrease of phase separation temperature upon the addition of  $\beta$ B1 to the solution. We determined the ratio of the effective energy of the  $\gamma$ D- $\beta$ B1 interaction, to that of the  $\gamma$ D- $\gamma$ D interaction:  $E_{12}/E_{11} = 0.7$ . We also determined the relative entropic contribution  $((dE_{11}/dT)T/E_{11} = -1.0 \pm 0.2)$  to the effective energy of the  $\gamma$ D- $\gamma$ D interaction. With these two parameters our thermodynamic analysis describes quantitatively the principle features of the phase behavior of this ternary protein solution. The reduction of phase separation temperature in the presence of  $\beta$ B1 suggests the importance of this protein in maintaining lens transparency.

**Table 2. Molecular latent heat,  $q$ , of LLPS of  $\gamma$ D-water binary solution calculated at several  $\phi^{\text{I}}$**

$\phi^{\text{I}}$	0.030	0.040	0.050	0.060	0.071
$-q/kT_c$	11.6	10.4	9.4	8.5	7.7
$N_A q$ (kJ/mol)	-26.8	-24.0	-21.6	-19.6	-17.7

## Materials and Methods

**Expression, Purification, and Characterization of Human  $\gamma$ D and  $\beta$ B1.** Recombinant human  $\gamma$ D and  $\beta$ B1 crystallins were prepared by amplification of the coding sequence from a human fetal lens cDNA library and were expressed in *Escherichia coli*, as described in our previous studies (8, 25). Overexpression and purification of  $\gamma$ D and  $\beta$ B1 were carried out as described previously (8, 25). The final products were analyzed by electrospray ionization mass spectrometry (ESI-MS model LCQ, ThermoQuest), which confirmed the molecular masses of 20,607 g/mol for  $\gamma$ D and 27,892 g/mol for  $\beta$ B1.

**Solution Preparation.** The purified  $\gamma$ D and  $\beta$ B1 proteins were dialyzed exhaustively into sodium phosphate buffer (0.1 M, pH 7.1) that contained sodium azide (0.02%) and DTT (20 mM). Solutions containing dilute  $\gamma$ D and  $\beta$ B1 in phosphate buffer were concentrated by ultrafiltration (Amicon, 10 kDa) and centrifugation (Amicon Ultra, 10 kDa). The concentrations of  $\gamma$ D and  $\beta$ B1 in the solutions were determined using a HPLC system (System Gold I26, Beckman Coulter) with a UV detector and a reverse phase column (Jupiter 5 $\mu$  C18 300A, phenomenex). Reverse phase HPLC was precalibrated with standard  $\gamma$ D and  $\beta$ B1 solutions without DTT. The concentrations of standard solutions were measured by an UV spectrometer at 280 nm using the extinction coefficient value of 2.09 mg<sup>-1</sup> · mL · cm<sup>-1</sup> for  $\gamma$ D and 2.06 mg<sup>-1</sup> · mL · cm<sup>-1</sup> for  $\beta$ B1 ([www.expasy.org](http://www.expasy.org)). Protein volume fractions in solution were calculated by multiplying the mass concentration by the specific volume of protein, 0.71 mL/mg (15).

**Measurement of  $T_{ph}$ .** A test tube containing the sample was placed in a thermostated light-scattering stage, whose temperature was initially set above  $T_{ph}$  so that the solution was transparent. The transmitted intensity of a 4-mW He-Ne laser was recorded by a photodiode. The temperature of the sample was then step wise lowered by 0.1 K every 5 min. At a well defined temperature,  $T_{cloud}$ , the sample became visibly cloudy. The temperature was then step wise raised by 0.1 K every 5 min. The minimum temperature at which the solution became clear again was denoted by  $T_{clarify}$ . The phase separation temperature  $T_{ph}$  is estimated as the average of  $T_{clarify}$  and  $T_{cloud}$ .

The difference between  $T_{cloud}$  and  $T_{clarify}$  is hysteresis which reflects the nucleation rate (14, 15). Since hysteresis depends on kinetic processes, all the cooling and heating steps were set with a standard time interval (5 min). In pure  $\gamma$ D solutions with  $\phi$  lower than 0.1, sedimentation of the protein-rich phase occurs in a time small compared to 5 min. In this domain we chose  $T_{ph}$  to be equal to  $T_{cloud}$ .

**Measurement of  $\gamma$ D- $\beta$ B1 Partitioning.** The solutions having known  $\phi$  and  $x$  were quenched to a temperature below  $T_{ph}$  in a thermostated water bath. After an incubation time of one week, a sharp interface formed between two liquid phases. The formation of the sharp interface was taken as an indication that equilibrium was reached. The  $\gamma$ D and  $\beta$ B1 crystallins in both phases were separated and their concentrations were measured using reverse phase HPLC. Using these concentrations we calculated  $\phi$  and  $x$  in each of the two coexisting phases.

**Quasielastic Light Scattering.** All protein samples were filtered through a 0.02  $\mu$ m Millipore filter and placed in a test tube. QLS experiments were performed on a light-scattering apparatus using a PD2000DLS<sup>PLUS</sup> correlator (Precision Detectors) and a Coherent He-Ne laser (35 mW, 632.8 nm; Coherent Radiation). The measurements were performed at a scattering angle of 90°. The measured correlation functions were analyzed by the Precision Deconvolve 5.5 software (Precision Detectors). The correlation functions were used to calculate the apparent diffusion coefficients,  $D$ , of proteins in solutions with given  $\phi$  and  $x$ .  $D(\phi = 0)_x$  were obtained by extrapolating  $D(\phi)_x$  to  $\phi = 0$ . The hydrodynamic radii,  $R_h$ 's, of proteins in solutions with fixed  $x$  were calculated from  $D(\phi = 0)_x$  using Stokes-Einstein relation.

**ACKNOWLEDGMENTS.** We acknowledge Dr. Nicolette Lubsen (Nijmegen Center for Molecular Life Sciences, Nijmegen, The Netherlands) for providing the original human  $\gamma$ D and  $\beta$ B1 clones for all of our work and Dr. Onofrio Annunziata and Dr. Ajay Pande for helpful discussions. This work was supported by National Institutes of Health Grants EY05127 (to G.B.B.).

- Bloemendal H, et al. (2004) Ageing and vision: structure, stability and function of lens crystallins. *Prog Biophys Mol Biol* 86:407–485.
- Hoehenwarter W, Klose J, Jungblut PR (2006) Eye lens proteomics. *Amino Acids* 30:369–389.
- Siezen RJ, Thomson JA, Kaplan ED, Benedek GB (1987) Human lens gamma-crystallins: isolation, identification, and characterization of the expressed gene products. *Proc Natl Acad Sci USA* 84:6088–6092.
- Benedek GB (1971) Theory of transparency of the eye. *Appl Optics* 10:459–473.
- Delaye M, Tardieu A (1983) Short-range order of crystallin proteins accounts for eye lens transparency. *Nature* 302:415–417.
- Gunton JD, Shirayev A, Pagan DL (2007) *Protein condensation: kinetic pathways to crystallization and disease* (Cambridge University Press, Cambridge, New York).
- Benedek GB (1997) Cataract as a protein condensation disease: the Proctor Lecture. *Invest Ophthalm Vis Sci* 38:1911–1921.
- Annunziata O, et al. (2005) Oligomerization and phase transitions in aqueous solutions of native and truncated human beta B1-crystallin. *Biochemistry* 44:1316–1328.
- Basak A, et al. (2003) High-resolution X-ray crystal structures of human gammaD crystallin (1.25 Å) and the R58H mutant (1.15 Å) associated with aculeiform cataract. *J Mol Biol* 328:1137–1147.
- McManus JJ, et al. (2007) Altered phase diagram due to a single point mutation in human gammaD-crystallin. *Proc Natl Acad Sci USA* 104:16856–16861.
- Pande A, et al. (2000) Molecular basis of a progressive juvenile-onset hereditary cataract. *Proc Natl Acad Sci USA* 97:1993–1998.
- Stephan DA, et al. (1999) Progressive juvenile-onset punctate cataracts caused by mutation of the gammaD-crystallin gene. *Proc Natl Acad Sci USA* 96:1008–1012.
- Talla V, Narayanan C, Srinivasan N, Balasubramanian D (2006) Mutation causing self-aggregation in human gammaC-crystallin leading to congenital cataract. *Invest Ophthalm Vis Sci* 47:5212–5217.
- Liu C, et al. (1996) Phase separation in aqueous solutions of lens gamma-crystallins: special role of gamma s. *Proc Natl Acad Sci USA* 93:377–382.
- Liu CW, et al. (1995) Phase-separation in multicomponents aqueous-protein solutions. *J Phys Chem* 99:454–461.
- Thomson JA, Schurtenberger P, Thurston GM, Benedek GB (1987) Binary liquid phase separation and critical phenomena in a protein/water solution. *Proc Natl Acad Sci USA* 84:7079–7083.
- Asherie N, Lomakin A, Benedek GB (1996) Phase diagram of colloidal solutions. *Phys Rev Lett* 77:4832–4835.
- Stradner A, Foffi G, Dorsaz N, Thurston G, Schurtenberger P (2007) New insight into cataract formation: enhanced stability through mutual attraction. *Phys Rev Lett* 99:198103.
- Dorsaz N, Thurston GM, Stradner A, Schurtenberger P, Foffi G (2009) Colloidal characterization and thermodynamic stability of binary eye lens protein mixtures. *J Phys Chem B* 113:1693–1709.
- Lampi KJ, et al. (1998) Age-related changes in human lens crystallins identified by two-dimensional electrophoresis and mass spectrometry. *Exp Eye Res* 67:31–43.
- Jung J, Byeon IJ, Wang Y, King J, Gronenborn A (2009) The structure of the cataract causing P23T mutant of HgD crystallin exhibits local distinctive conformational and dynamic changes. *Biochemistry* 48:2597–2609.
- Van Montfort RL, Bateman OA, Lubsen NH, Slingsby C (2003) Crystal structure of truncated human betaB1-crystallin. *Protein Sci* 12:2606–2612.
- Broide ML, Berland CR, Pande J, Ogun OO, Benedek GB (1991) Binary-liquid phase separation of lens protein solutions. *Proc Natl Acad Sci USA* 88:5660–5664.
- Lomakin A, Asherie N, Benedek GB (1996) Monte Carlo study of phase separation in aqueous protein solutions. *J Chem Phys* 104:1646–1656.
- Pande A, et al. (2001) Crystal cataracts: human genetic cataract caused by protein crystallization. *Proc Natl Acad Sci USA* 98:6116–6120.
- ten Wolde PR, Frenkel D (1997) Enhancement of protein crystal nucleation by critical density fluctuations. *Science* 277:1975–1978.
- Jones HC, Pfeffer W, Raoult FM, Hoff JHvt, Arrhenius S (1899) *The modern theory of solution; memoirs by Pfeffer, van't Hoff, Arrhenius, and Raoult* (Harper, New York, London), pp x, p 133.
- Carnahan NF, Starling KE (1969) Equation of state for nonattracting rigid spheres. *J Chem Phys* 51:635–636.
- Lomakin A, Asherie N, Benedek GB (1999) Aeolotopic interactions of globular proteins. *Proc Natl Acad Sci USA* 96:9465–9468.
- Leonard PJ, Henderso D, Barker JA (1970) Perturbation theory and liquid mixtures. *T Faraday Soc* 66:2439–2452.
- Landau LD, Lifshits EM, Pitaevskii LP (1980) *Statistical physics* (Pergamon Press, Oxford, New York), 3d rev. and enl. Ed.
- Friberg G, Pande J, Ogun O, Benedek GB (1996) Pantethine inhibits the formation of high-Tc protein aggregates in gamma B crystallin solutions. *Curr Eye Res* 15:1182–1190.
- Benedek GB, Pande J, Thurston GM, Clark JI (1999) Theoretical and experimental basis for the inhibition of cataract. *Prog Retin Eye Res* 18:391–402.